

## Determining $\gamma$ from $B \rightarrow \pi\pi$ Decays without the $CP$ -Asymmetry $C_{\pi^0\pi^0}$

Christian W. Bauer,<sup>1</sup> Ira Z. Rothstein,<sup>2</sup> and Iain W. Stewart<sup>3</sup>

<sup>1</sup>California Institute of Technology, Pasadena, California 91125, USA

<sup>2</sup>Department of Physics, Carnegie Mellon University, Pittsburgh, Pennsylvania 15213, USA

<sup>3</sup>Center for Theoretical Physics, Massachusetts Institute of Technology, Cambridge, Massachusetts 02139, USA

(Received 23 December 2004; published 17 June 2005)

Factorization based on the soft-collinear effective theory (SCET) can be used to reduce the number of hadronic parameters in an isospin analysis of  $B \rightarrow \pi\pi$  decays by one. This gives a theoretically precise method for determining the  $CP$  violating phase  $\gamma$  by fitting to the  $B \rightarrow \pi\pi$  data without  $C_{\pi^0\pi^0}$ . SCET predicts that  $\gamma$  lies close to the isospin bounds. With the current world averages we find  $\gamma = 75^\circ \pm 2^{+9}_{-13}$ , where the uncertainties are theoretical, then experimental.

DOI: 10.1103/PhysRevLett.94.231802

PACS numbers: 12.15.Hh, 11.30.Er, 12.39.Hg, 13.25.Hw

Measurements of  $CP$  violation are an important tool to look for physics beyond the standard model (SM) [1]. Standard model measurements of  $CP$  violation in  $B$  decays are usually expressed in terms of the angles  $\alpha$ ,  $\beta$ , and  $\gamma$ . To test the SM picture of  $CP$  violation, one looks for inconsistencies by making measurements in as many decay channels as possible.

Important observables for measuring  $\gamma$  (or  $\alpha$ ) are the  $CP$  asymmetries and branching fractions in  $B \rightarrow \pi\pi$  decays. Unfortunately, hadronic uncertainties and ‘‘penguin pollution’’ make the data difficult to interpret. Gronau and London (GL) [2] have shown that using isospin,  $\text{Br}(\bar{B} \rightarrow \pi^+\pi^-)$ ,  $\text{Br}(B^+ \rightarrow \pi^+\pi^0)$ ,  $\text{Br}(\bar{B} \rightarrow \pi^0\pi^0)$ , and the  $CP$  asymmetries  $C_{\pi^+\pi^-}$ ,  $S_{\pi^+\pi^-}$ ,  $C_{\pi^0\pi^0}$ , one can eliminate the hadronic uncertainty and determine  $\gamma$ . This year *BABAR* and *Belle* Collaborations [3] reported the first observation of  $C_{\pi^0\pi^0}$ . Unfortunately, the uncertainties in  $C_{\pi^0\pi^0}$  and  $\text{Br}(B \rightarrow \pi^0\pi^0)$  are still too large to give strong constraints, leaving a fourfold discrete ambiguity and a  $\pm 29^\circ$  window of uncertainty in  $\gamma$  (at  $1\sigma$ ) near the SM preferred value.

In this Letter we observe that the soft-collinear effective theory (SCET) [4] predicts that one hadronic parameter vanishes at leading order in a power expansion in  $\Lambda_{\text{QCD}}/E_\pi$ , and that this provides a robust new method for determining  $\gamma$  using the experimental value of  $\beta$ . The parameter is  $\epsilon = \text{Im}(C/T)$ , where  $T$  and  $C$  are defined below and are predominantly ‘‘tree’’ and ‘‘color suppressed tree’’ amplitudes. From [5] we know that  $\epsilon$  vanishes to all orders in  $\alpha_s(\sqrt{E_\pi\Lambda_{\text{QCD}}})$  since the ‘‘jet function’’ does not involve a strong phase, and so  $\epsilon$  receives corrections suppressed by  $\Lambda_{\text{QCD}}/E_\pi$  or  $\alpha_s(m_b)$ . Our method *does not rely* on a power expansion for any of the other isospin parameters. Thus, issues like the size of charm penguin diagrams and whether ‘‘hard-scattering’’ or ‘‘soft’’ contributions dominate the  $B \rightarrow \pi$  form factors [5–11] are irrelevant here. Our results are sufficiently robust to allow for the so-called ‘‘chirally enhanced’’ power corrections [7]. The method differs from the QCD

factorization (QCDF) [7] and perturbative QCD [11] analyses; for example, we work to all orders in  $\Lambda_{\text{QCD}}/m_b$  for most quantities and do not use QCD sum rule inputs.

The world averages for the  $CP$  averaged branching ratios ( $\overline{\text{Br}}$ ) and the  $CP$  asymmetries are [3,12]

	$\overline{\text{Br}} \times 10^6$	$C_{\pi\pi}$	$S_{\pi\pi}$
$\pi^+\pi^-$	$4.6 \pm 0.4$	$-0.37 \pm 0.11$	$-0.61 \pm 0.13$
$\pi^0\pi^0$	$1.51 \pm 0.28$	$-0.28 \pm 0.39$	
$\pi^+\pi^0$	$5.61 \pm 0.63$		

For later convenience we define the ratios

$$\begin{aligned}\bar{R}_c &= \frac{\overline{\text{Br}}(B^0 \rightarrow \pi^+\pi^-)\tau_{B^-}}{2\overline{\text{Br}}(B^- \rightarrow \pi^0\pi^-)\tau_{B^0}} = 0.446 \pm 0.064, \\ \bar{R}_n &= \frac{\overline{\text{Br}}(B^0 \rightarrow \pi^0\pi^0)\tau_{B^-}}{\overline{\text{Br}}(B^- \rightarrow \pi^0\pi^-)\tau_{B^0}} = 0.293 \pm 0.064,\end{aligned}\quad (1)$$

and quote the product  $\bar{R}_n C_{\pi^0\pi^0} = 0.082 \pm 0.116$ .

To obtain general expressions for these observables, we use isospin and unitarity of the Cabibbo-Kobayashi-Maskawa (CKM) matrix to write

$$\begin{aligned}A(\bar{B}^0 \rightarrow \pi^+\pi^-) &= e^{-i\gamma}|\lambda_u|T - |\lambda_c|P \\ &\quad + (e^{-i\gamma}|\lambda_u| - |\lambda_c|)P_{\text{ew}}^1, \\ A(\bar{B}^0 \rightarrow \pi^0\pi^0) &= e^{-i\gamma}|\lambda_u|C + |\lambda_c|P \\ &\quad + (e^{-i\gamma}|\lambda_u| - |\lambda_c|)(P_{\text{ew}}^2 - P_{\text{ew}}^1), \\ \sqrt{2}A(B^- \rightarrow \pi^0\pi^-) &= e^{-i\gamma}|\lambda_u|(T + C) \\ &\quad + (e^{-i\gamma}|\lambda_u| - |\lambda_c|)P_{\text{ew}}^2.\end{aligned}\quad (2)$$

Here  $\lambda_u = V_{ub}V_{ud}^*$ ,  $\lambda_c = V_{cb}V_{cd}^*$ . The  $CP$  conjugate amplitudes are obtained from (2) with  $\gamma \rightarrow -\gamma$ .  $T$ ,  $C$ ,  $P$ , and the electroweak penguin amplitudes  $P_{\text{ew}}^{1,2}$  are complex.

The amplitude  $P_{\text{ew}}^2$  is related to  $T$  and  $C$  by isospin [13]. An additional relation for  $P_{\text{ew}}^1$  can be obtained using SCET at lowest order in  $\Lambda/E_\pi$  and  $\alpha_s(m_b)$  [5]. For the numerically dominant coefficients  $C_{9,10}$  we find

$$\begin{aligned}
P_{\text{ew}}^1 &= e_1 T + e_2 C, & P_{\text{ew}}^2 &= e_3 T + e_4 C, \\
e_1 &= \frac{C_{10}(C_1 - C_3) + C_9(C_4 - C_2)}{(C_1 + C_2)(C_1 - C_2 - C_3 + C_4)} = -9.5 \times 10^{-5}, \\
e_2 &= \frac{C_9(C_1 + C_4) - C_{10}(C_2 + C_3)}{(C_1 + C_2)(C_1 - C_2 - C_3 + C_4)} = -9.0 \times 10^{-3}, \\
e_3 &= e_4 = \frac{3}{2}(C_9 + C_{10})(C_1 + C_2)^{-1} = -1.4 \times 10^{-2},
\end{aligned} \tag{3}$$

with  $C_i$  from the electroweak Hamiltonian. Since  $e_3|T|/|P| = e_3(p_s^2 + p_c^2)^{-1/2}|\lambda_c|/|\lambda_u| \sim 0.06$  for typical values of the parameters  $p_s$  and  $p_c$  (from below), we estimate that the electroweak penguin diagrams give at most a  $\sim 6\%$  correction to any amplitude. It would be easy to include  $P_{\text{ew}}^{1,2}$ , but for simplicity we neglect them in what follows. SCET allows contributions from  $C_7$  and  $C_8$  to be included in (3), giving  $e_3 = -1.5 \times 10^{-2}$  and  $e_4 = -1.3 \times 10^{-2}$ .

Of the five remaining isospin parameters, one,  $|\lambda_u(T+C)|$ , is fixed by  $\text{Br}(B^- \rightarrow \pi^0 \pi^-)$  and just sets the overall scale. We choose the remaining four parameters as

$$\begin{aligned}
p_c &\equiv -\frac{|\lambda_c|}{|\lambda_u|} \text{Re}\left(\frac{P}{T}\right), & p_s &\equiv -\frac{|\lambda_c|}{|\lambda_u|} \text{Im}\left(\frac{P}{T}\right), \\
t_c &\equiv \frac{|T|}{|T+C|}, & \epsilon &\equiv \text{Im}\left(\frac{C}{T}\right).
\end{aligned} \tag{4}$$

The parameters  $p_c$  and  $p_s$  determine the size of the ‘‘penguin’’ contribution  $P$  relative to the tree  $T$ , and the parameters  $t_c$  and  $\epsilon$  determine the shape of the isospin triangle as shown in Fig. 1. The relations to parameters used previously [5,14] are  $r_c^2 = p_c^2 + p_s^2$  and  $\tan \delta_c = p_s/p_c$ .

In terms of the parameters in (4) the observables can be written as (neglecting electroweak penguin diagrams)

$$\begin{aligned}
S_{\pi^+\pi^-} &= -[\sin(2\beta + 2\gamma) + 2\sin(2\beta + \gamma)p_c + \sin(2\beta) \\
&\quad \times (p_c^2 + p_s^2)][1 + 2p_c \cos \gamma + p_c^2 + p_s^2]^{-1}, \\
C_{\pi^+\pi^-} &= \frac{2p_s \sin \gamma}{1 + 2p_c \cos \gamma + p_c^2 + p_s^2}, \\
\bar{R}_c &= t_c^2(1 + 2p_c \cos \gamma + p_c^2 + p_s^2), \\
\bar{R}_n &= (1 - t_c)^2 + t_c^2(p_c^2 + p_s^2) - 2t_c(1 - t_c)p_c \cos \gamma \\
&\quad - \epsilon(2t_c^2 p_s) \cos \gamma \\
&\quad + [1 \mp \sqrt{1 - \epsilon^2 t_c^2}]2t_c(1 + p_c \cos \gamma), \\
\bar{R}_n C_{\pi^0 \pi^0} &= 2t_c \sin \gamma [t_c p_s \mp p_s \sqrt{1 - \epsilon^2 t_c^2} + \epsilon p_c t_c].
\end{aligned} \tag{5}$$

The  $\mp$  signs in the last two equations should be chosen to be the same, and correspond to whether the apex of the triangle in Fig. 1(a) is to the right or left of the  $(0,0)$  point. Since both  $|\lambda_c|$  and  $|\lambda_u|$  are absorbed into the hadronic parameters  $p_s$  and  $p_c$ , there is no added uncertainty from  $|V_{ub}|$ . For the CKM angle  $\beta$  we use the latest average [1,12],  $\beta = 23.3^\circ \pm 1.5^\circ$ .

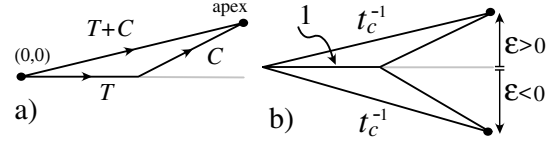


FIG. 1. (a) Isospin triangle in the  $|\lambda_u|$  sector, and (b) the scaled triangle with solutions for positive and negative  $\epsilon$  shown.

The full isospin analysis requires solving the five Eqs. (5) to obtain the parameters  $p_c$ ,  $p_s$ ,  $t_c$ , and  $\epsilon$  defined in (4) and the weak angle  $\gamma$ . From  $S_{\pi^+\pi^-}$  and  $C_{\pi^+\pi^-}$  one obtains two solutions for the parameters  $p_s$  and  $p_c$  as functions of the angle  $\gamma$ . Using these,  $\bar{R}_c$  determines  $t_c(\gamma)$ . Finally,  $\bar{R}_n$  and  $\bar{R}_n C_{\pi^0 \pi^0}$  each give two quadratic equations for  $\epsilon$ , which in general have four intersections in the  $\epsilon - \gamma$  plane. We call  $\epsilon_{1,2}$  the two solutions from  $\bar{R}_n$  and  $\epsilon_{3,4}$  the two solutions from  $\bar{R}_n C_{\pi^0 \pi^0}$ . An example of this GL isospin analysis is shown in Fig. 2, where we use the current central values for the data. For illustration we picked the solution for  $p_c$  and  $p_s$  with  $|P/T| < 1$ , but have shown all four  $\epsilon_i$ 's.

An obvious feature in Fig. 2 is the isospin bounds on  $\gamma$ . It is well known that there are bounds on  $\gamma$  in the absence of a measurement of  $C_{\pi^0 \pi^0}$  [15]. To find these analytically, one defines  $\gamma = \pi - \beta - \alpha_{\text{eff}} + \theta$  where

$$\begin{aligned}
\sin(2\alpha_{\text{eff}}) &= S_{\pi\pi}(1 - C_{\pi\pi}^2)^{-1/2} = -0.66 \pm 0.14, \\
\cos(2\theta) &\geq (\bar{R} - 1)(1 - C_{\pi\pi}^2)^{-1/2} = 0.53 \pm 0.19,
\end{aligned} \tag{6}$$

with  $\bar{R} = (1 + \bar{R}_c - \bar{R}_n)^2 / (2\bar{R}_c)$ . The four solutions are

$$\begin{aligned}
-163.0^\circ \leq \gamma \leq -105.0^\circ, & & -31.8^\circ \leq \gamma \leq 26.3^\circ, \\
17.1^\circ \leq \gamma \leq 75.2^\circ, & & 148.0^\circ \leq \gamma \leq 206.0^\circ,
\end{aligned} \tag{7}$$

with uncertainty  $\pm 8.2^\circ$  on each limit. At each of these bounds the two solutions  $\epsilon_{1,2}$  become degenerate, and beyond they are complex, indicating that the isospin triangle does not close.

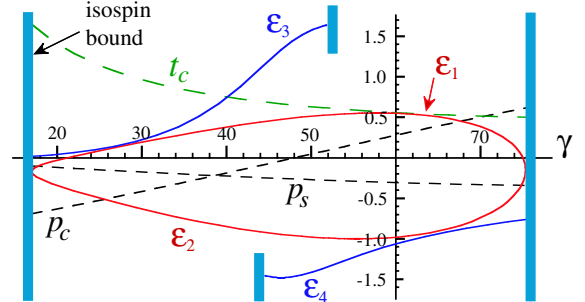


FIG. 2 (color online). Isospin analysis showing the hadronic parameters  $\{p_c, p_s, t_c, \epsilon\}$  versus  $\gamma$  using current central values of the  $B \rightarrow \pi\pi$  data. Solutions for  $\gamma$  occur at crossings of the  $\epsilon_i$  curves. Experimental uncertainties are not shown, and are especially large for  $\epsilon_{3,4}$ . This plot shows only one of two allowed  $(p_c, p_s)$  solutions and one of the two allowed  $\gamma$  regions.

Solutions for  $\gamma$  from the GL isospin analysis are given where the curves  $\epsilon_{3,4}$  intersect the curves  $\epsilon_{1,2}$ . There are up to four solutions within each isospin bound, which are symmetric around  $\gamma_{\text{eff}} = \pi - \beta - \alpha_{\text{eff}}$ . We show in Fig. 2 the results for  $17.1^\circ \leq \gamma \leq 75.2^\circ$ . The current central values  $\epsilon_{3,4}$  do not intersect  $\epsilon_{1,2}$ , and in the absence of experimental uncertainties there would be no solution for  $\gamma$ . The current central values for the observables are such that the solutions for  $\epsilon$  from  $\bar{R}_n$  and  $\bar{R}_n C_{\pi^0 \pi^0}$  are almost tangential. Including experimental uncertainties, a large range of  $\gamma$  is allowed, with the highest confidence at  $\gamma = 27^\circ$  and  $\gamma = 65^\circ$ . This conclusion agrees with the CKMfitter group's analysis which incorporates  $C_{\pi^0 \pi^0}$  [16].

Using SCET at LO in  $\alpha_s(m_b)$  and  $\Lambda_{\text{QCD}}/m_b$  we have  $\epsilon = 0$  [5], which corresponds to flat isospin triangles in Fig. 1. Equivalently

$$\epsilon \sim \mathcal{O}\left(\frac{\Lambda_{\text{QCD}}}{m_b}, \alpha_s(m_b)\right). \quad (8)$$

Neglecting EW penguin diagrams,  $\epsilon$  is a renormalization group equation invariant quantity since Eq. (5) fixes it in terms of observables. Equation (8) makes an extraction of  $\gamma$  from  $B \rightarrow \pi\pi$  possible without needing precision data on  $C_{\pi^0 \pi^0}$ . In this method the central values for  $\gamma$  are determined by finding the places where the  $\epsilon_1$  and/or  $\epsilon_2$  curves cross the  $x$  axis, meaning we solve  $\epsilon_{1,2}(\gamma) = 0$ . The other hadronic parameters,  $p_c$ ,  $p_s$ , and  $t_c$  are determined in the same way as in the isospin analysis. This proposal for determining  $\gamma$  using Eq. (8) is the main result of this Letter.

Using the central values for all the data besides  $C_{\pi^0 \pi^0}$  and solving  $\epsilon_{1,2}(\gamma) = 0$  gives the solutions

$$\gamma = -159^\circ, -105^\circ, 21.5^\circ, 74.9^\circ. \quad (9)$$

We have four solutions rather than the eight of the isospin analysis [which occur within the first and third isospin bounds in (7)], because factorization for the  $B \rightarrow \pi\pi$  amplitudes resolves the discrete ambiguity in  $p_s$  and  $p_c$  in favor of  $|P/T| < 1$  solutions [this follows from the factorization for light-quark penguin diagrams, the size of Wilson coefficients, charm velocity power counting, and factors of  $\alpha_s(m_c)$  [5,7]]. Next we analyze the theoretical and experimental uncertainties in our method for  $\gamma$ , and contrast these with the isospin analysis, focusing on the two solutions that can occur in the  $17.1^\circ \leq \gamma \leq 75.2^\circ$  region preferred by global fits for the unitarity triangle [16].

To estimate the theoretical uncertainty we take

$$-0.2 \leq \epsilon \leq 0.2, \quad (10)$$

which corresponds to roughly a 20% effect from perturbative or power corrections. We also consider a much more pessimistic scenario where this range is doubled to  $\epsilon = \pm 0.4$ . Note that  $|\epsilon| < 0.2$  can accommodate the so-called ‘‘chirally enhanced’’ power corrections, which have been argued to dominate [7]. Using the results from Ref. [7], including known  $\alpha_s(m_b)$  and power corrections, we randomly scan the two complex parameters  $X_A$  and  $X_H$  in their

default range to find  $|\epsilon| = |\text{Im}(C/T)|_{\text{QCDF}} = -0.05 \pm 0.04$ . This is below the uncertainty assigned to our analysis.

In Fig. 3 we show  $\epsilon_{1,2}$  for the region  $65^\circ < \gamma < 78^\circ$ . Here the solution is  $\gamma = 74.9^\circ$ , and the different shading corresponds to the theory uncertainty with  $|\epsilon| < 0.2(0.4)$ . The solution for  $\gamma$  is very close to the isospin bound, so the upward uncertainty on  $\gamma$  is very small. (The uncertainty in the isospin bound is contained in the experimental uncertainty.) For the downward uncertainty we consider the overlap with the shaded region. For  $|\epsilon| < 0.2$  we find  $\Delta\gamma_{\text{theo}} = {}^{+0.3^\circ}_{-1.5^\circ}$ , while for  $|\epsilon| < 0.4$  we find  $\Delta\gamma_{\text{theo}} = {}^{+0.3^\circ}_{-5.2^\circ}$ . On top of that there are uncertainties from hadronic isospin violation, typically  $\lesssim 3\%$ , which we take to be  $\pm 2^\circ$ . (A slightly larger  $\sim 5^\circ$  uncertainty was found in [17], but using a smaller penguin amplitude. Larger isospin violation can be accounted for by scaling up the  $\pm 2^\circ$  lower bound on our theory error.) Thus, with perfect data at the current central values we arrive at a theory uncertainty with  $|\epsilon| < 0.2$  as  $\Delta\gamma_{\text{theo}} = \pm 2^\circ$ . Repeating for the smaller solution at  $\gamma = 21.5^\circ$ , we find a larger theory uncertainty,  $\Delta\gamma_{\text{theo}} = {}^{+8.7^\circ}_{-4.4^\circ}$ , since the  $\epsilon_{1,2}$  curves are flatter near this solution.

To determine the  $1\sigma$  experimental errors, we use the program MINUIT. Taking  $\epsilon = 0$  and fitting to  $\gamma$  and the four hadronic parameters, we find

$$\gamma = 21.5^\circ {}^{+9.4^\circ}_{-7.9^\circ}, \quad \gamma = 74.9^\circ {}^{+8.1^\circ}_{-10.6^\circ}. \quad (11)$$

These uncertainties are purely experimental and are propagated with the assumption that the original input data are uncorrelated. If we instead set  $\epsilon = 0.2$ , then we find  $\gamma = 73.3^\circ {}^{+8.8^\circ}_{-13.3^\circ}$  and  $\gamma = 30.7^\circ {}^{+11.1^\circ}_{-7.2^\circ}$ , whereas fixing  $\epsilon = -0.2$  gives  $\gamma = 75.2^\circ {}^{+7.6^\circ}_{-9.5^\circ}$  and  $\gamma = 17.2^\circ {}^{+8.7^\circ}_{-6.9^\circ}$ . Combining these numbers we obtain our final result for  $\gamma$  including all sources of uncertainty

$$\gamma = 74.9^\circ \pm 2^\circ {}^{+9.4^\circ}_{-13.3^\circ}. \quad (12)$$

Here the first error is theoretical, and the last errors are experimental where we picked the largest range obtained in varying  $\epsilon = \pm 0.2$ . The theory error increases to  $\Delta\gamma = {}^{+2^\circ}_{-5.2^\circ}$  for the more pessimistic case  $\epsilon = \pm 0.4$ . The analog of (12) for the lower solution is  $\gamma = 21.5^\circ {}^{+8.7^\circ}_{-4.4^\circ} {}^{+11.1^\circ}_{-7.9^\circ}$ .

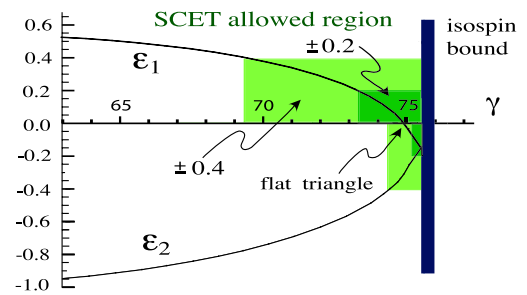


FIG. 3 (color online). Regions of  $\gamma$  preferred by our analysis. The shaded areas show our best estimate of the theoretical uncertainty from power corrections,  $-0.2 \leq \epsilon \leq 0.2$  as well as the pessimistic estimate  $-0.4 \leq \epsilon \leq 0.4$ . Experimental uncertainties are not shown.

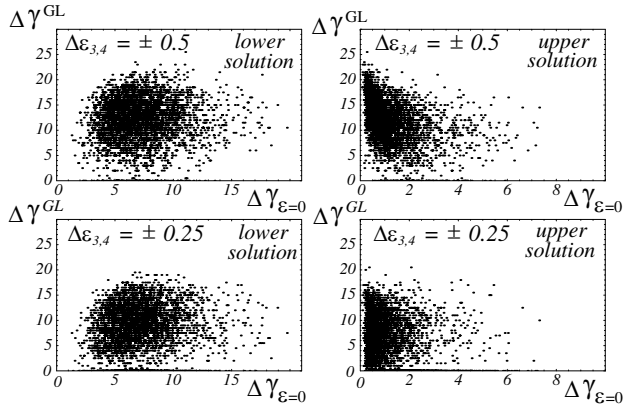


FIG. 4. Uncertainty in the isospin analysis from  $C_{\pi^0\pi^0}$  ( $y$  axis) vs theoretical uncertainty from our new method ( $x$  axis). The upper (lower) two plots use a  $\pm 0.5$  ( $\pm 0.25$ ) uncertainty in  $\epsilon_{3,4}$ . The plots on the left (right) correspond to the solution near the lower (upper) isospin bound.

The analysis presented here relies on the fact that a small value of  $|\epsilon|$  is allowed only for a narrow range of  $\gamma$ . While this is certainly true given the current central values of the data, it is instructive to investigate how the quality of the analysis is affected if the data central values change. For example, it could be that the value of  $\epsilon_1$  never exceeds 0.2, increasing the uncertainties from the small- $\epsilon$  analysis significantly. A second extreme situation is that  $\epsilon$  never reaches zero. To study these questions, we generate random sets of data using Gaussian distributions with the current central values and width of the  $1\sigma$  uncertainties. We generate 10 000 sets of “data,” and after imposing  $\sin(2\alpha_{\text{eff}}) < 1$  and  $\cos(2\theta) < 1$  are left with 9688 sets. Of these, 96% have solutions for  $\epsilon = 0$ . For  $\epsilon_1$  we find 88% (70%) of the sets have the maximum value above 0.2 (0.4). It is only for these data sets that our analysis works. For  $\epsilon_2$  we find that  $\sim 100\%$  of the sets have their minimum below  $-0.4$ . Thus, the small  $\epsilon$  analysis works in most cases.

We can also study the uncertainty in our analysis, compared to the GL isospin analysis. Rather than performing a full error analysis for the 9688 sets, we use the following approximation. We assume that experimental uncertainty  $\Delta C_{\pi^0\pi^0}$  dominates, and compare the resulting uncertainty in the GL isospin analysis to the theoretical uncertainty in our analysis, for cases where values of  $\gamma$  exist with  $\epsilon > 0.2$  as discussed above. The current  $\Delta C_{\pi^0\pi^0} = \pm 0.39$  gives rise to a  $\Delta\epsilon_{3,4} \sim \pm 0.5$ . In Fig. 4 we show the uncertainties in the GL analysis compared with the theoretical uncertainties of the analysis presented here, for both solutions of  $\gamma$ . The plots use 4000 points. If we take  $\Delta\epsilon_{3,4} \sim \pm 0.25$ , the GL analysis still has uncertainties in  $\gamma$  that are considerably larger than the small  $\epsilon$  analysis. We also see that the  $\pm 2^\circ$  error quoted in (12) is typical.

We have presented a new method for obtaining  $\gamma$  from  $B \rightarrow \pi\pi$  decays without  $C_{\pi^0\pi^0}$ . Our analysis uses SCET to eliminate one hadronic parameter. The theory uncertainty

for a solution  $\gamma = 74.9^\circ$  is small,  $\pm 2$  or  ${}^{+2}_{-5.2}^\circ$ , depending on the estimate for power corrections. Analyzing possible future shifts in the data and decreases in the  $C_{\pi^0\pi^0}$  uncertainty, we find that this method should have smaller uncertainty than the isospin analysis for quite some time. The analysis can be redone including the electroweak penguin diagrams. Obviously agreement between *BABAR* and *Belle* on  $S_{\pi^+\pi^-}$  and  $C_{\pi^+\pi^-}$  is needed before one will have complete trust in the  $\gamma$  from  $B \rightarrow \pi\pi$ .

We thank D. Pirjol for collaboration in early stages of this Letter and Z. Ligeti and J. Zupan for comments on the manuscript. This work was supported in part by the DOE under DE-FG03-92ER40701, DOE-ER-40682-143, DEAC02-6CH03000, and the cooperative research agreement DF-FC02-94ER40818. I. S. is also supported by the Office of Nuclear Science, the DOE OJI program, and the Sloan Foundation.

- [1] For a recent review see Z. Ligeti, hep-ph/0408267.
- [2] M. Gronau and D. London, Phys. Rev. Lett. **65**, 3381 (1990).
- [3] Y. Chao *et al.*, Phys. Rev. Lett. **94**, 181803 (2005); **93**, 021601 (2004); B. Aubert *et al.* (*BABAR* Collaboration), hep-ex/0408081; hep-ex/0408089.
- [4] C. Bauer *et al.*, Phys. Rev. D **63**, 014006 (2001); **63**, 114020 (2001); C. Bauer and I. Stewart, Phys. Lett. B **516**, 134 (2001); C. Bauer *et al.*, Phys. Rev. D **65**, 054022 (2002); **66**, 014017 (2002).
- [5] C. W. Bauer, D. Pirjol, I. Z. Rothstein, and I. W. Stewart, Phys. Rev. D **70**, 054015 (2004).
- [6] J. g. Chay and C. Kim, Phys. Rev. D **68**, 071502 (2003); Nucl. Phys. **B680**, 302 (2004).
- [7] M. Beneke *et al.*, Phys. Rev. Lett. **83**, 1914 (1999); M. Beneke and M. Neubert, Nucl. Phys. **B675**, 333 (2003).
- [8] M. Ciuchini *et al.*, Nucl. Phys. **B501**, 271 (1997); Phys. Lett. B **515**, 33 (2001); P. Colangelo *et al.*, Z. Phys. C **45**, 575 (1990).
- [9] T. Feldmann and T. Hurth, J. High Energy Phys. **11** (2004) 037.
- [10] A. Szczepaniak *et al.*, Phys. Lett. B **243**, 287 (1990).
- [11] Y. Y. Keum *et al.*, Phys. Lett. B **504**, 6 (2001); Phys. Rev. D **63**, 054008 (2001); C. D. Lu *et al.*, Phys. Rev. D **63**, 074009 (2001).
- [12] HFAG, <http://www.slac.stanford.edu/xorg/hfag/>.
- [13] M. Neubert and J. L. Rosner, Phys. Rev. Lett. **81**, 5076 (1998); M. Neubert, J. High Energy Phys. **02** (1999) 014; M. Gronau *et al.*, Phys. Rev. D **60**, 034021 (1999); A. J. Buras and R. Fleischer, Eur. Phys. J. C **11**, 93 (1999).
- [14] A. J. Buras *et al.*, Phys. Rev. Lett. **92**, 101804 (2004); A. Ali *et al.*, Eur. Phys. J. C **36**, 183 (2004); C. W. Chiang *et al.*, Phys. Rev. D **70**, 034020 (2004).
- [15] Y. Grossman and H. R. Quinn, Phys. Rev. D **58**, 017504 (1998); J. Charles, Phys. Rev. D **59**, 054007 (1999); M. Gronau *et al.*, Phys. Lett. B **514**, 315 (2001).
- [16] J. Charles *et al.* (CKMfitter Collaboration), hep-ph/0406184.
- [17] S. Gardner, Phys. Rev. D **59**, 077502 (1999).